Solar Energy Materials & Solar Cells 95 (2011) 2933–2936

Contents lists available at ScienceDirect

Solar Energy Materials & Solar Cells

journal homepage: www.elsevier.com/locate/solmat

Letter

Nondestructive local analysis of current–voltage characteristics of solar cells by lock-in thermography

Otwin Breitenstein *

Max Planck Institute of Microstructure Physics, Weinberg 2, D-06120 Halle, Germany

ARTICLE INFO

Article history:
Received 4 April 2011
Accepted 27 May 2011
Available online 14 June 2011

Keywords:
Solar cells
Local analysis
Dark IV characteristics
Lock-in thermography

ABSTRACT

By evaluating dark lock-in thermography images taken at one reverse and three forward biases, images of all two-diode-parameters J_{01}, J_{02}, n (ideality factor of J_{02}), and G_p (the parallel Ohmic conductivity) of the dark current–voltage characteristic are obtained. A local series resistance is explicitly considered and may be provided as a series resistance image, e.g. resulting from luminescence imaging. The results enable a separate investigation of factors influencing the depletion region recombination current and the diffusion current, which is governed by the bulk lifetime. Local I–V characteristics of special sites may be simulated.

1. Introduction

The dark current of pn-junctions can be described by the 2-diode model, comprising two exponential contributions (e= electron charge, kT=thermal energy, V=bias) [1]:

$$J(V)=J_{01}\left(\exp\frac{eV}{kT}-1\right)+J_{02}\left(\exp\frac{eV}{nkT}-1\right)=J_{diff}(V)+J_{rec}(V) \qquad (1)$$

In solar cells additionally an Ohmic parallel resistance R_p and a series resistance R_s have to be regarded. The first term in Eq. (1) is the so-called "diffusion current" $J_{diff}(V)$ described by its saturation current density J_{01}, which is a measure of all recombination processes in the bulk and in the emitter volume and dominates at high forward bias, and the second term is the depletion region "recombination current" $J_{rec}(V)$ described by its saturation current density J_{02} and ideality factor n, which is due to recombination in the depletion region of the pn-junction and dominates at low forward bias. If the lifetime is independent on minority carrier concentration, the ideality factor of the diffusion current is always 1. Very often, within a limited bias range, these two contributions are combined as one exponential current density described by an "effective" saturation current density J_0 and an ideality factor n. Dark lock-in thermography (DLIT) allows one to image the forward current density quantitatively and, by evaluating images taken at two forward biases, even allows to image the local "effective" J_0- and n-distribution [2,3]. In silicon, DLIT at a forward bias of about 0.5 V images predominantly the J_{02}- and at 0.6 V it images predominantly the J_{01}-contribution. However, these are always "mixed" images, hence even at 0.5 V contributions of J_{01} and at 0.6 V contributions of J_{02} are visible in the images. Since certain recombination centers may influence J_{01}, J_{02}, and n in a different way, a separate imaging of both contributions would be highly desirable for a deeper understanding of the local recombination behavior. The purpose of this work is to develop a method, which allows a separate imaging of all three relevant dark current parameters J_{01}, J_{02}, and n, thereby J_{diff} and J_{rec}, and of the Ohmic parallel conductance $G_p=1/R_p$ (R_p=parallel resistance). Note that here all resistances are defined area-related in units of $\Omega\,cm^2$.

An attempt to regard both the diffusion and the local (depletion region) recombination current for interpreting the global current–voltage (I–V) characteristic was made in [4]. However, for obtaining an analytical solution, quite drastic simplifications have been used there. Thus, it was assumed that the J_{01}-distribution is described by an effective ideality factor larger than 1 and is strictly homogeneous. This was not a separate imaging of J_{diff}- and J_{rec}-contributions over the whole area, which will be performed in this work.

2. Materials and methods

The solar cells used for these investigations were a commercial multicrystalline and an experimental monocrystalline cell in standard technology (screen-printed contacts, full area Al back contact). The lock-in thermography investigations were performed using a Thermosensorik system [5]. All evaluations and simulations were performed using a specially developed code called "Local I–V".

* Tel.: +49 345 5582740; fax: +49 345 5511223.
E-mail address: breiten@mpi-halle.mpg.de

0927-0248/$ - see front matter © 2011 Elsevier B.V. All rights reserved.
doi:10.1016/j.solmat.2011.05.049

3. Theory/calculation

Like most other quantitative LIT methods, this technique is based on the fact that, within a limited spatial resolution given by the thermal diffusion length, the $-90°$ component of the DLIT image $T^{-90°}(x,y)$ can be scaled in units of the locally dissipated power density [3,6] by applying ($<T^{-90°}(x,y)>$ = average value of $T^{-90°}(x,y)$, P = total dissipated power, A = cell area):

$$p(x,y) = \frac{T^{-90°}(x,y)P}{<T^{-90°}(x,y)>A} \tag{2}$$

A special and necessary feature of the method described here is that it explicitly regards the area-related series resistance $R_s(x,y)$ to each position (x,y), given in units of $\Omega\,cm^2$, which either may be assumed to be position-independent or may be imported from an independent imaging method like EL/PL imaging [7] or RESI [8]. Then the local bias $V(x,y)$ is the applied bias V_B minus the voltage drop at the local series resistance $R_s(x,y)$. Thus, neglecting the power dissipation due to the voltage drop in the sheet resistance, the locally dissipated power density $p(x,y)$ can be expressed as

$$p(x,y) = V(x,y)J(x,y) = [V_B - J(x,y)R_s(x,y)]J(x,y) \tag{3}$$

This can be resolved to

$$J(x,y) = \frac{V_B}{2R_s(x,y)} - \sqrt{\frac{V_B^2}{4R_s(x,y)^2} - \frac{p(x,y)}{R_s(x,y)}} \tag{4}$$

For R_s approaching zero, $J(x,y) = p(x,y)/V_B$ follows from Eq. (3), as expected. Knowing $J(x,y)$ and $R_s(x,y)$, now the local voltage $V(x,y)$ may be calculated for any bias voltage V_B using Eq. (3). Note that this approach neglects the Joule heat dissipated at the emitter series resistance due to horizontal current flow. Thus, if an extended high-R_s area existed in a solar cell, the inside region of this area should be treated correctly, but in its edge region, where most of the Joule heat is dissipated in the emitter, some errors may occur. The same approximation was made for the RESI method for imaging local series resistances [8].

Now the influence of Ohmic shunting is regarded. It is assumed that the DLIT image taken at a weak reverse bias V_{Brev} (typically -1 V) contains only the Ohmic contribution, leading to

$$G_p(x,y) = \frac{J_{rev}(x,y)}{V_{Brev}(x,y)} \tag{5}$$

Now the remaining local two-diode-parameters $J_{01}(x,y)$, $J_{02}(x,y)$, and $n(x,y)$ are obtained from DLIT results measured at three forward biases V_{B1}, V_{B2}, and V_{B3} (typically 0.5, 0.55, and 0.6 V). Since this problem cannot be solved analytically, an iteration procedure is used. The basic idea of this procedure is to calculate n and J_{02} from the measurements at V_{B1} and V_{B2} with the J_{01}- and G_p-contributions being a correction, and to calculate J_{01} from the measurement at V_{B3} with the J_{02}- and G_p-contributions being a correction. As a first approximation we neglect the diffusion current contribution at V_{B1} and V_{B2}, i.e. starting values $J_{01}^0(x,y)=0$ are used for all positions (x,y). Using the notation in Eq. (1) and for

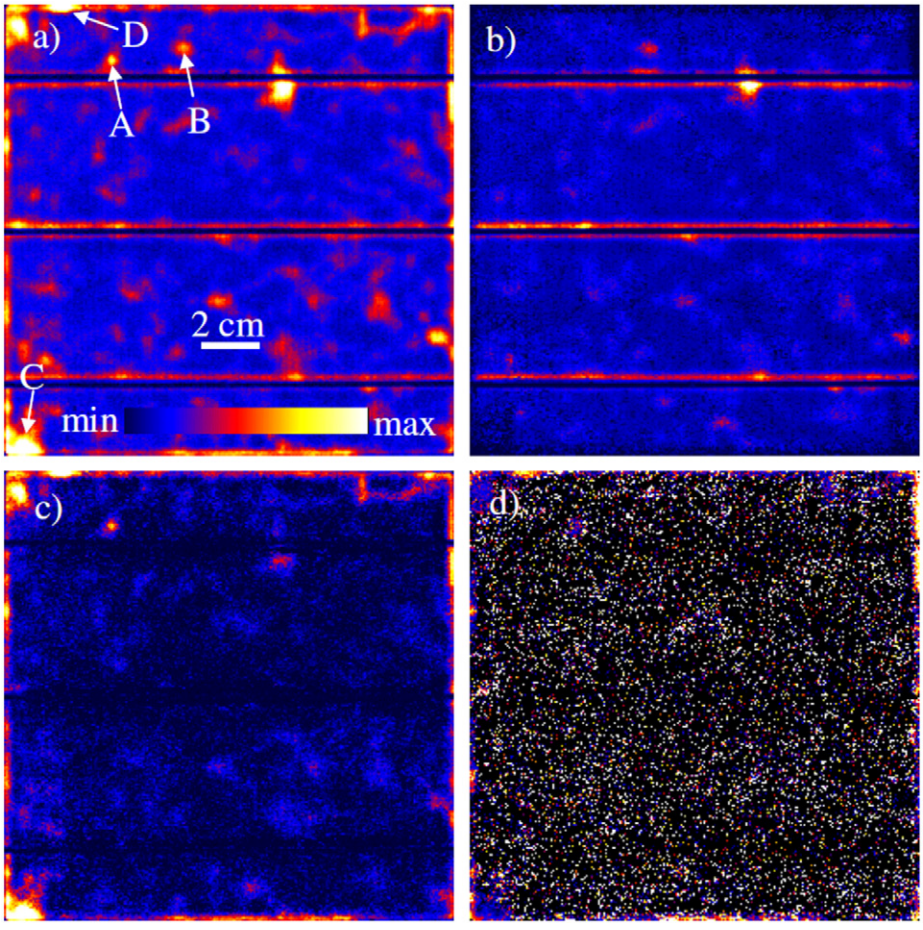

Fig. 1. (a) Measured current density, (b) diffusion current density, and (c) recombination current density at +0.55 V of a multicrystalline cell, all in the same scaling, (d) ideality factor scaled from 1.5 to 5.

the Ohmic contribution $J_G(x,y,V)=G_p(x,y)^*V(x,y)$, the iteration implies the following steps (e=electron charge, kT=thermal energy, m=iteration counter, beginning with $m=1$):

$$n^m(x,y)=\frac{\frac{e}{kT}(V_2(x,y)-V_1(x,y))}{\ln\left(\frac{J_2(x,y)-{J_{diff}}^{m-1}(x,y,V_2)-J_G(x,y,V_2)}{J_1(x,y)-{J_{diff}}^{m-1}(x,y,V_1)-J_G(x,y,V_1)}\right)} \quad (6)$$

$${J_{02}}^m(x,y)=\frac{J_2(x,y)-{J_{diff}}^{m-1}(x,y,V_2)-J_G(x,y,V_2)}{\exp\left(\frac{eV_2(x,y)}{n^m(x,y)kT}\right)} \quad (7)$$

$${J_{01}}^m(x,y)=\frac{J_3(x,y)-{J_{rec}}^m(x,y,V_3)-J_G(x,y,V_3)}{\exp\left(\frac{eV_3(x,y)}{kT}\right)} \quad (8)$$

Eqs. (6)–(8) have to be calculated repeatedly with up-counting iteration counter m. After about 20 iterations a self-consistent solution for $J_{01}(x,y)$, $J_{02}(x,y)$, and $n(x,y)$ is obtained. This whole procedure is implemented in a code called "Local *I–V*", which is available from the author.

The analysis of many global and local *I–V* characteristics of solar cells leads to $n>2$ [3,4,6,9], which cannot be explained by standard point defect recombination theory. Therefore, and for obtaining a generalized value for J_{02}, many authors fit the characteristics using a fixed ideality factor of $n=2$, even if the curve fit is not exact. This simplification can be made also here by skipping Eq. (6) and setting all n-values to 2. Note that in this special case the problem can be solved even analytically. This

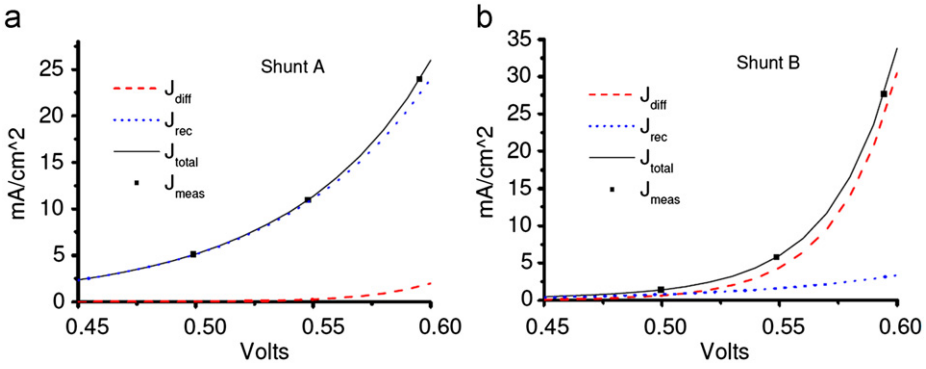

Fig. 2. Separation of the currents of two shunts A and B into "diffusion current" and "recombination current" contributions.

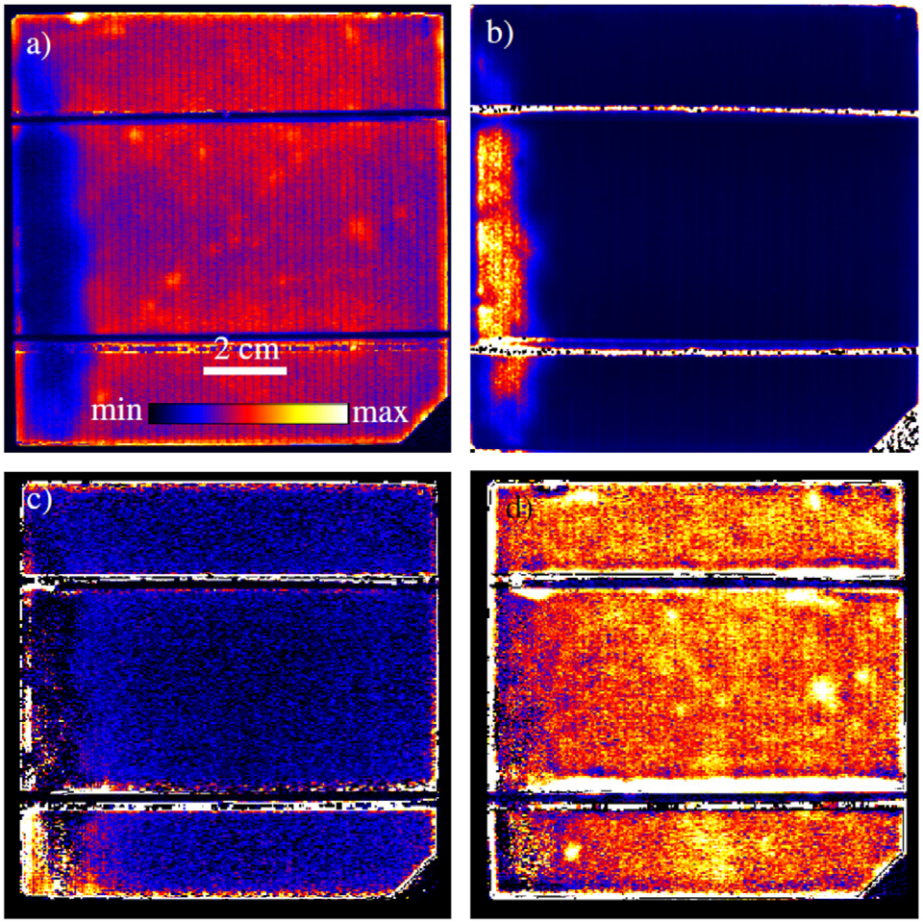

Fig. 3. (a) DLIT image at 0.6 V of a monocrystalline cell with R_s problems [a.u], (b) R_s image (measured by RESI [7]) used for evaluation, scaled to 20 Ω cm^2, (c) J_{01} scaled from 0 to 5×10^{-12} A/cm^2, (d) J_{02}, scaled from 0 to 2×10^{-7} A/cm^2.

option is also implemented in the "Local *I–V*" code, leading to the same results as the iterative procedure introduced here.

4. Results

The complete iteration method with variable ideality factor was first applied to a $156 \times 156\ mm^2$ sized commercial multicrystalline solar cell. This cell did not contain any Ohmic shunts and had a very low series resistance. $V_{Brev} = -1$ V, $V_{B1} = 0.5$ V, $V_{B2} = 0.55$ V, and $V_{B3} = 0.6$ V have been used and a constant R_s of $0.2\ \Omega cm^2$ was assumed. Fig. 1 (a) shows the measured current density map of this cell at 0.55 V calculated according to Eq. (4), (b) shows the diffusion current density J_{diff} and (c) the recombination current density J_{rec}, all for $V_B = 0.55$ V in the same scaling, and (d) shows the ideality factor map scaled from 1.5 to 5. The measured current density maps and the current density maps simulated from the calculated J_{01}-, J_{02}-, n-, and G_p-distributions were virtually indistinguishable for all four biases. Fig. 1 shows, e.g. that the increased current density around the bus bars is a pure J_{01}-effect, which is due to the higher backside surface recombination velocity at the silver contact stripes at the back. On the other hand, the increased current density in the edge regions is a pure recombination current. Point shunt "A" is due to depletion region recombination and "B" due to bulk recombination. The ideality factor image (d) is very noisy in most of the area, since it also relies on the 0.5 V DLIT image (not shown here) where the current density in the area was very weak. Nevertheless, in the regions of strong recombination current the values of n are significant. Thus, in region "C" $n = 2.4$ and in "D" (at the upper edge) $n = 4.2$ was measured, whereas in most of the area an average value of $n \approx 2$ holds. It had been shown previously that ideality factors larger than two may be caused by recombination via extended defects [9]. By evaluating the local 2-diode parameters, also *I–V* characteristics for selected regions may be calculated and compared with each other, which is demonstrated for shunts A and B in Fig. 2.

In a second example, the method was applied to a $125 \times 125\ mm^2$ sized experimental monocrystalline cell suffering from inhomogeneous series resistance and a large recombination current due to a previous Corescan investigation. Fig. 3(a) shows the DLIT image taken at 0.6 V and (b) the series resistance image used in Eq. (4) coming from a RESI investigation [8]. Here $n = 2$ was assumed for the evaluation. While in Fig. 1 the (bias-dependent) diffusion and recombination currents were shown, Fig. 3(c) and (d) show the J_{01}- and J_{02}-distributions of this cell, respectively. In spite of the strong DLIT signal dip in the high-R_s region, these two parameters appear nearly homogeneous (especially J_{02}, which is the dominating current contribution here), apart from the increased noise in this region, as expected for a monocrystalline cell. This proves that this method is indeed able to regard the influence of a variable series resistance in the calculation of local p–n junction parameters, if this resistance is known. As for the multicrystalline cell of Fig. 1, the recombination current, reflected by J_{02}, is increased in the edge region.

5. Discussion/conclusions

This method can be expected to become a valuable tool for local analysis of dark *I–V* characteristics of solar cells and for looking at physical limitations for J_{01} and J_{02}. While J_{01} is governed by the lifetime in the bulk, J_{02} and n are governed by recombination in the depletion region. As discussed in [9], the origin of this recombination are mostly locally extended defects (including the edge) leading to a high local density of recombination states. These states are obviously more effective for depletion region recombination than for bulk recombination. A qualitative argument for this is the fact that J_{01} increases with reducing lifetime τ with $1/\sqrt{\tau}$ while J_{02} decreases with $1/\tau$ [1]. Thus, regions with extremely low lifetime increase J_{02} stronger than J_{01}. The method introduced here may help to study such effects in more detail.

Acknowledgment

The author is indebted to D. Reinke (Sunways, Arnstadt) for providing the industrial multicrystalline cell, to A. van der Heide (formerly ECN, Petten) for providing the monocrystalline cell, to K. Iwig (MSC Technik, Halle) for writing the "Local *I–V*" code, and to J. Müller and K. Bothe (ISFH, Hameln) for performing the R_s-imaging by RESI.

References

[1] S.M. Sze, Kwok K. Ng, Physics of Semiconductor Devices, third ed., Wiley, Hoboken NJ, 2007, pp. 90–98.
[2] O. Breitenstein, M. Langenkamp, J.P. Rakotoniaina, J. Zettner, The imaging of shunts in solar cells by infrared lock-in thermography, in: Proceedings of the 17th European PVSEC, Munich 2001, pp. 1499–1502.
[3] O. Breitenstein, J.P. Rakotoniaina, M.H. Al Rifai, Quantitative evaluation of shunts in solar cells by lock-in thermography, Prog. Photovolt.: Res. Appl. 11 (2003) 515–526.
[4] O. Breitenstein, A. Khanna, W. Warta, Quantitative description of dark current–voltage characteristics of multicrystalline solar cells based on lock-in thermography measurements, Phys. Status Solidi A 207 (2010) 2159–2163.
[5] ⟨www.thermosensorik.de⟩.
[6] O. Breitenstein, W. Warta, M. Langenkamp, Lock-in Thermography—Basics and Use for Evaluating Electronic Devices and Materials, second ed., Springer, Berlin/Heidelberg, 2010, pp. 193–196.
[7] M. Glatthaar, J. Haunschild, M. Kasemann, J. Giesecke, W. Warta, S. Rein, Spatially resolved determination of dark saturation current and series resistance of silicon solar cells, Phys. Status Solidi RRL 4 (2010) 13–15.
[8] K. Ramspeck, K. Bothe, D. Hinken, B. Fischer, J. Schmidt, R. Brendel, Recombination current and series resistance imaging of solar cells by combined luminescence and lock-in thermography, Appl. Phys. Lett. 90 (2007) 153502.
[9] O. Breitenstein, J. Bauer, P.P. Altermatt, K. Ramspeck, Influence of defects on solar cell characteristics, Solid State Phenom. 156–158 (2010) 1–10.